The Astrophysical Journal, 857:61 (5pp), 2018 April 10 https://doi.org/10.3847/1538-4357/aab36a

The First Laboratory Detection of Vibration-rotation Transitions of $^{12}CH^+$ and $^{13}CH^+$ and Improved Measurement of Their Rotational Transition Frequencies

José L. Doménech[1], Pavol Jusko[2,3], Stephan Schlemmer[2], and Oskar Asvany[2]
[1] Instituto de Estructura de la Materia (IEM-CSIC), Serrano 123, E-28006 Madrid, Spain
[2] I. Physikalisches Institut, Universität zu Köln, Zülpicher Str. 77, D-50937 Köln, Germany; asvany@ph1.uni-koeln.de
Received 2018 February 1; revised 2018 February 22; accepted 2018 February 26; published 2018 April 13

Abstract

C–H stretches of the fundamental ions CH^+ and $^{13}CH^+$, which have long been searched for, have been observed for the first time in the laboratory. The state-dependent attachment of He atoms to these ions at cryogenic temperatures has been exploited to obtain high-resolution rovibrational data. In addition, the lowest rotational transitions of CH^+, $^{13}CH^+$ and CD^+ have been revisited and their rest frequency values have improved substantially.

Key words: ISM: molecules – methods: laboratory: molecular – molecular data

1. Introduction

Methylidynium, CH^+, was the first molecular ion and one of the first interstellar molecules observed in space, through its absorption lines in the visible region (Dunham 1937). It was identified in the laboratory by Douglas & Herzberg (1941). Since then, it has proven to be almost ubiquitous, and it has been observed in different environments through its electronic transitions, both in emission (see, e.g., Hobbs et al. 2004) and absorption (see, e.g., Weselak et al. 2008) in the Milky Way, and also in other galaxies (Welty et al. 2006). The observation of the CH^+ $J = 1-0$ rotational transition at ~835 GHz from the ground, however, is hindered by a strong telluric oxygen line. One way out is the observation of the $^{13}CH^+$ isotopologue at ~830 GHz, which has been detected with the CSO and APEX telescopes under very good weather conditions (Falgarone et al. 2005; Menten et al. 2011), or the observation of CH^+ in redshifted extragalactic sources in the millimeter-wave region, as detected with ALMA toward the blazar PKS 1830−211 (Muller et al. 2017) and a group of starburst galaxies (Falgarone et al. 2017). Local observations of the rotational lines of CH^+ require satellite missions. Cernicharo et al. (1997) observed pure rotational transitions in emission with the *ISO* satellite, and *Herschel* has provided extensive data both in absorption against bright submillimeter sources (e.g., Falgarone et al. 2010; Godard et al. 2012) and in emission in warm gas environments (e.g., Nagy et al. 2013; Parikka et al. 2017).

The astrophysical relevance of CH^+ stems from its role as an initiator and key molecule in the carbon chemistry in the interstellar medium, and from its yet to be understood, high abundance in diffuse clouds. This is a problem that has puzzled astronomers since the 70s (Dalgarno 1976), because the observed abundances in diffuse clouds are well above the values predicted by even the most recent models (e.g., Valdivia et al. 2017 and references therein). The main formation reaction is believed to be the reaction $C^+ + H_2 \rightarrow CH^+ + H$, which is endothermic (by 0.37 eV, or ~4300 K) when H_2 is in its ground vibrational state (Hierl et al. 1997). Therefore, in order to surmount the formation barrier in diffuse clouds, different sources of suprathermal energy have been suggested, like C-shocks (Flower & Pineau des Forets 1998), magnetohydrodynamic shocks (Lesaffre et al. 2013), or turbulent dissipation (Godard et al. 2014). These processes could favor the formation of CH^+ and overcome the efficient destruction mechanisms of CH^+, mainly reactions with H and H_2 and recombination with electrons. In warmer environments like PDRs in dense clouds, the vibrational excitation of H_2 makes the formation reaction above exothermic, proceeding at almost the Langevin rate (Agúndez et al. 2010; Zanchet et al. 2013).

Despite its astrophysical importance, accurate laboratory data on its rotational spectrum did not become available until very recently (Amano 2010a; Yu et al. 2015). Most previously available information came from the electronic emission spectrum of the $A^1\Pi$–$X^1\Sigma$ system, the most notable experiments being those of Carrington & Ramsay (1982) and Hakalla et al. (2006) on $^{12}CH^+$, and those of Bembenek et al. (1987) and Bembenek (1997a, 1997b) on $^{13}CH^+$, $^{12}CD^+$, and $^{13}CD^+$, respectively. The astronomical observation by Cernicharo et al. (1997) was of too low resolution for an accurate determination of the lowest-frequency transitions, and a previous laboratory measurement of the $J = 1-0$ transition of $^{12}CH^+$ (Pearson & Drouin 2006) was proven to be too low by 58 MHz. Amano (2010a) finally provided accurate frequencies for that transition, as well as for $^{13}CH^+$ and $^{12}CD^+$. In contrast, the vibration-rotation IR spectrum had eluded observation until now. Prior to the work described here, the rovibrational lines of $^{12}CH^+$ were also searched for with a difference frequency spectrometer coupled to a hollow cathode discharge (Cueto et al. 2014; Doménech et al. 2016) without success, thus emphasizing the elusive character of the vibration-rotation spectrum of this fundamental ion, already pointed out by Rehfuss et al. (1992). An exhaustive compilation of the spectroscopic laboratory literature, used in a direct potential fit of all available frequency data, can be found in Cho & Le Roy (2016).

Regarding transition intensities, Follmeg et al. (1987) calculated the permanent electrical dipole moment of CH^+ to be $\mu_0 = 1.679$ D, and the transition dipole moment for the $v = 1-0$ band $\mu_{1-0} = 0.016$ D. These values are in reasonable agreement with those derived from Sauer & Špirko (2013) of 1.7 D and 0.0196 D, respectively. Cheng et al. (2007) calculated $\mu_0 = 1.683$ D, but they did not derive a vibrational

[3] Current affiliation: Institut de Recherche en Astrophysique et Planétologie (IRAP), Université de Toulouse (UPS), CNRS, CNES, 9 Av. du Colonel Roche, 31028 Toulouse Cedex 4, France.

transition moment. The low value of μ_{1-0}, together with the high reactivity of CH^+, which is rapidly destroyed by collisions with H_2, O_2, or H_2O typically present in discharge tubes as traces, could explain the non-observation in the cold cathode experiments.

In this work, we present the first direct observation of vibration-rotation lines of $^{12}CH^+$ and $^{13}CH^+$, with accuracies better than 1 MHz, as well as significantly improved measurements of the $J = 1-0$ rotational transitions already available.

2. Experimental Setup

The spectroscopy of CH^+ was facilitated by a cryogenic ion trap experiment, in which the mentioned parasitic reactants are frozen out. As the applied trapping setup (Asvany et al. 2010, 2014) and the action schemes for rovibrational, as well as pure rotational spectroscopy, have been thoroughly documented by Asvany et al. (2014), Savić et al. (2015), Jusko et al. (2016, 2017), Doménech et al. (2017), Stoffels et al. (2016), and Brünken et al. (2014, 2017), only a brief description is given here. The CH^+ (similarly $^{13}CH^+$ and CD^+) ions have been generated in a storage ion source by bombarding the precursor gas (CH_4 Linde 5.5, $^{13}CH_4$ Sigma Aldrich 99%, or CD_4 Cambridge Isotope Laboratories 99%, respectively) with electrons (with energies in the range 30–40 eV). A pulse of about ten-thousand mass-selected ions was injected into the 22-pole ion trap filled with about 10^{14} cm^{-3} He. During the trapping time of 700 ms, the complexes CH^+–$(He)_n$ ($n = 1$–4) formed by three-body collisions. The detection of the resonant absorption of the continuous radiation (submillimeter or IR) by the naked ion was achieved by observing the decrease of complexes with $n = 1$ (masses 17 u or 18 u, respectively). The IR radiation was provided by an Aculight Argos Model 2400 cw OPO (optical parametric oscillator), with the power in the trap reaching hundreds of mW. The frequency of the IR radiation has been measured by our frequency comb system (Asvany et al. 2012) with an accuracy in the range of 80 kHz. The submillimeter-wave radiation was supplied by a synthesizer driving a multiplier chain source (Virginia Diodes, Inc.) covering the range 80–1100 GHz. The nominal submillimeter-wave power at the frequency of the fundamental rotational transition of CH^+ was about 6 μW. Both the used synthesizer (Agilent E8257D) and the frequency comb system were locked to a rubidium atomic clock (with a typical stability of 10^{-11}).

3. Rovibrational and Rotational Transitions

The low temperature requirement of our spectroscopy method (with a a maximum operation temperature of about 20 K for the CH^+–He case), together with the large rotational constants of these light hydrides allowed us to investigate only a few low-lying transitions in this work (albeit with very high precision). We based our search on the available accurate predictions for the $^1\Sigma$ ground state provided by Müller (2010), Yu et al. (2016), and the CDMS database (Endres et al. 2016). For the isotopologues CH^+ and $^{13}CH^+$, four rovibrational transitions and one rotational transition have been found and recorded, and are summarized in Tables 1 and 2. Whereas the IR transitions are detected for the first time in this work, the pure rotational lines have been measured before by Amano (2010a) and Yu et al. (2015) in a discharge cell, and their values are also included in the tables. Interestingly, in our IR scans we also observed rovibrational transitions of the complex CH^+–He (and similarly $^{13}CH^+$–He), which are detected by their photodissociation upon absorption. These lines can be distinguished by their lifetime-broadened Lorentzian shape and their spectral position; see Figure 1. This is very similar to the observations made for the H_3^+–He system by Savić et al. (2015), for which both the naked ion and its He complex have been observed in the same spectrum. The spectrum of CH^+–He will be analyzed in a future publication.

Table 1
Measured Frequencies of Rotational and Rovibrational Transitions of CH^+, and Comparison to Former Work

$(v, J) \leftarrow (v, J)$	This Work	Former Work	Unit
(0, 1) ← (0, 0)	835137.4408(10)	835137.504(20)[a]	MHz
(0, 2) ← (0, 1)		1669281.361(100)[b]	MHz
(0, 3) ← (0, 2)		2501443.102(100)[b]	MHz
(1, 0) ← (0, 1)	2711.812948(22)		cm^{-1}
(1, 1) ← (0, 0)	2766.548226(6)		cm^{-1}
(1, 2) ← (0, 1)	2792.414725(7)		cm^{-1}
(1, 3) ← (0, 2)	2817.237730(65)		cm^{-1}

Notes. The accuracy of our measurements is given by locking the frequency comb and the millimeter-wave synthesizer to a rubidium clock. The narrow Doppler widths lead to relative precisions close to 1 ppb. Every line in this table has been measured at least five times, with the final error given in parentheses.
[a] Amano (2010a).
[b] Yu et al. (2015).

Table 2
Measured Frequencies of Rotational and Rovibrational Transitions of $^{13}CH^+$, and Comparison to Former Work

$(v, J, F) \leftarrow (v, J, F)$	This Work	Former Work	Unit
$(0, 1, \frac{1}{2}) \leftarrow (0, 0, \frac{1}{2})$	830214.9715(23)	830215.004(30)[a]	MHz
$(0, 1, \frac{3}{2}) \leftarrow (0, 0, \frac{1}{2})$	830216.5505(10)	830216.640(30)[a]	MHz
(0, 2) ← (0, 1)		1659450.286(100)[b]	MHz
(0, 3) ← (0, 2)		2486725.636(100)[b]	MHz
(1, 0) ← (0, 1)	2704.128959(27)		cm^{-1}
(1, 1) ← (0, 0)	2758.544719(3)		cm^{-1}
(1, 2) ← (0, 1)	2784.264862(9)		cm^{-1}
(1, 3) ← (0, 2)	2808.950977(38)		cm^{-1}

Notes. The two hyperfine components of the (0, 1) ← (0, 0) transition (due to the spin $I = 1/2$ of the ^{13}C nucleus) have been clearly separated in our cryogenic measurements. Every line in this table has been measured at least five times, with the final error given in parentheses.
[a] Amano (2010a).
[b] Yu et al. (2015).

An example of a pure rotational measurement is shown in Figure 2. We choose to show the $J = 1 \leftarrow 0$ transition of $^{13}CH^+$, as this transition can be observed from the ground (Falgarone et al. 2005; Menten et al. 2011), and because it exhibits the hyperfine structure first seen by Amano (2010a, 2010b) in the laboratory. The hyperfine splitting is clearly resolved in our cryogenic experiment with a 1:2 intensity ratio. For this rotational measurement, as well as for the rovibrational measurements of the CH^+ isotopologues, we generally detect pure Gaussian profiles with a measured Doppler temperature close to $T = 12$ K (with the ion trap at nominal 4 K). Additional power-broadening, as sometimes observed in trap-based millimeter-wave spectroscopy (see, e.g.,

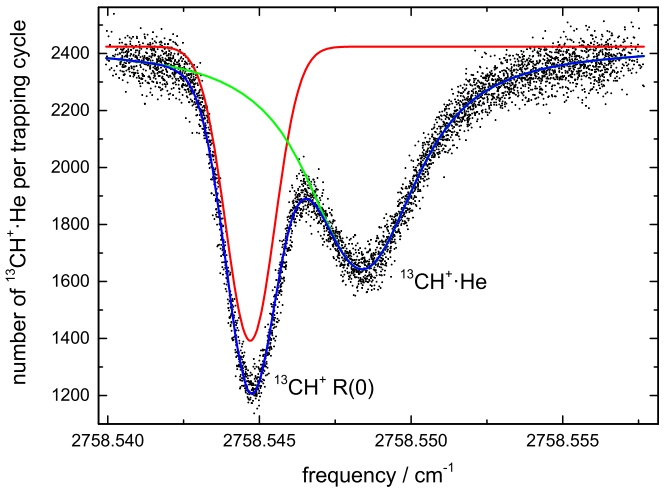

Figure 1. Accidental blending of the $R(0)$ transition of $^{13}CH^+$ with one unassigned transition of $^{13}CH^+$–He. We observe the state-dependent He-attachment to $^{13}CH^+$ and the predissociation line of $^{13}CH^+$–He simultaneously by counting the $^{13}CH^+$–He ions (mass 18 u) after the 700-ms trapping time during which the ions are irradiated. These two species can be distinguished by their spectral positions and their line shapes. The shown $^{13}CH^+$ line is Doppler-broadened and has a Gaussian shape (red), giving a temperature $T = 13$ K, while the $^{13}CH^+$–He line is additionally lifetime-broadened, with a Voigt profile (green). Its Lorentzian contribution yields a lifetime $\tau = 1.6$ ns of the vibrationally excited state.

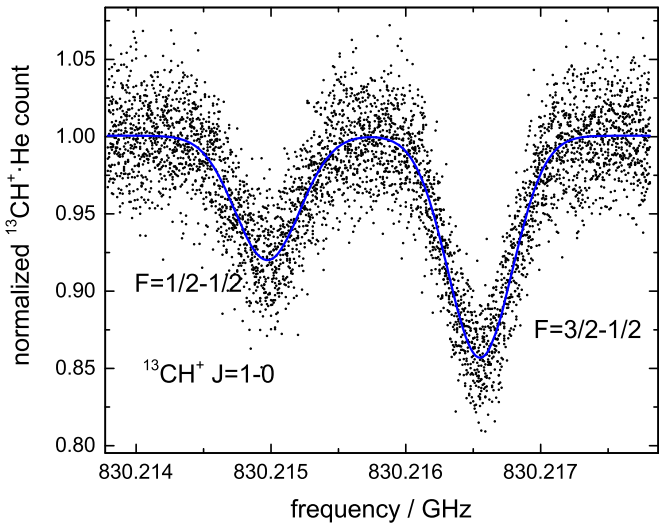

Figure 2. The $J = 1 \leftarrow 0$ rotational transition of $^{13}CH^+$ recorded at a nominal temperature of 4 K, showing two clearly resolved hyperfine components. Every ion count (black dot) has been normalized by a subsequent count with the submillimeter-wave source being off-resonant. The hyperfine structure is caused by the $I(^{13}C) = 1/2$ nuclear spin of the ^{13}C nucleus, whereas the influence of the hydrogen nuclear spin $I(H) = 1/2$ is negligible here: $F = J + I(^{13}C)$.

Töpfer et al. 2016; Brünken et al. 2017) is not observed here due to the limited power applied.

The fundamental rovibrational transitions of CD^+ were not accessible by our OPO system, but we revisited the two lowest rotational transitions, which are listed in Table 3. We could improve the value for the $J = 2 \leftarrow 1$ transition by nearly two orders of magnitude, while the accurate value for $J = 1 \leftarrow 0$ given very recently by Brünken et al. (2017; measured in the Cologne laboratories in a different trap setup) is confirmed.

Table 3
Measured Frequencies of Rotational Transitions of CD^+ with Comparison to Former Work

$(v, J) \leftarrow (v, J)$	This Work	Former Work	Unit
$(0, 1) \leftarrow (0, 0)$	453521.8530(6)	453521.8509(7)[a]	MHz
		453521.851(20)[b]	MHz
$(0, 2) \leftarrow (0, 1)$	906752.1649(17)	906752.156(100)[c]	MHz
$(0, 3) \leftarrow (0, 2)$		1359399.836(100)[c]	MHz
$(0, 4) \leftarrow (0, 3)$		1811173.908(100)[c]	MHz

Notes. The values are derived from typically 10 independent measurements. The final errors are given in parentheses.
[a] Brünken et al. (2017).
[b] Amano (2010a).
[c] Yu et al. (2015).

Table 4
The Best-fit Spectroscopic Parameters of CH^+ Are Obtained by Fitting the Data Given in Table 1 with the Program PGOPHER (Western 2017)

Parameter	$v = 0$	$v = 1$	Unit
ν		2739.670097(5)	cm^{-1}
B	417651.595(4)	402974.48(8)	MHz
D	41.451(2)	40.741(9)	MHz
H	0.0067(2)	0.0065	MHz

Note. To constrain the distortion constant H in the ground state, the high-J observations of Cernicharo et al. (1997) have also been used. For the vibrationally excited state, a scaled fixed value has been adopted for H. The numbers in parentheses give the uncertainty of the last digits.

Table 5
The Best-fit Spectroscopic Parameters of $^{13}CH^+$ Are Obtained by Fitting the Data Given in Table 2 with the Program PGOPHER (Western 2017)

Parameter	$v = 0$	$v = 1$	Unit
ν		2731.822034(8)	cm^{-1}
B	415189.908(1)	400643.48(14)	MHz
D	40.9609(7)	40.27(1)	MHz
H	0.0066	0.0064	MHz
C_I	1.053(1)		MHz

Note. For the distortion constants H, scaled fixed values have been adopted. The numbers in parentheses give the uncertainty of the last digits. The hyperfine spin-rotation coupling constant C_I has been calculated and measured previously by Sauer & Paidarová (1995) and Amano (2010b).

4. Results and Outlook

The submillimeter-wave frequencies given in Tables 1 through 3 compare very favorably with other work, the deviations being less than 3σ compared to our accurate values. Also, the predictions for the IR transitions given currently in the CDMS database (Endres et al. 2016) turned out to be very accurate, with a less than 0.01 cm^{-1} difference for the low-J CH^+ transitions given in Table 1. The frequencies available in Tables 1 and 2 have been used to determine the spectroscopic parameters in the ground and excited vibrational states. For CH^+, the known FIR transitions detected with the *ISO* satellite by Cernicharo et al. (1997) helped to constrain the distortion constants in the ground state. For $^{13}CH^+$, the well-resolved hyperfine components allow us to determine the spin-rotation coupling constant C_I with high precision. The obtained values can be found in Tables 4 and 5.

While the improvement of the rotational frequencies for the CH^+ isotopologues into the 1 ppb regime are only of limited impact for the interpretation of astronomical data, the measured rovibrational transitions open up their potential observation in the MIR regime. The low-lying vibration-rotation transitions measured in this work are in the range 3.5–3.7 μm and are thus accessible from the ground. Using the calculated vibrational transition dipole moment, and typical column densities and excitation temperatures derived from observations in the visible or millimeter-wave, one can estimate the peak absorptions that could be expected in an infrared observation. For example, Falgarone et al. (2010) derived a column density of $N = 1.7 \times 10^{14}$ molec cm^{-2}, an excitation temperature of 3 K, and velocity spreads of 5 km s^{-1} for the absorptions of CH^+ toward the massive star-forming region DR21. For those conditions, most of the population resides in $J = 0$, and the strongest IR absorption would be that of the $R(0)$ line at 2766.548226(6) cm^{-1} (3.6146 μm). With $\mu_{1-0} = 0.016$ D, the integrated line intensity is calculated to be

$$\int_{-\infty}^{+\infty} \alpha(\tilde{\nu}) d\tilde{\nu} = 3.0 \times 10^{-19} \text{ cm}^2 \text{ cm}^{-1} \text{ molec}^{-1}. \quad (1)$$

The observed peak absorption will be directly proportional to the column density N, and inversely proportional to the observed line width. Assuming the line width to be limited by the cloud velocity spread, and a triangular line shape, the FWHM is on the order of $5/299792 \times 2766.5 \text{ cm}^{-1} = 0.046 \text{ cm}^{-1}$ (that would imply using a spectrograph with a resolving power better than $R \sim 60{,}000$). The opacity at the line center (or, equivalently, the peak absorption) would then be

$$\alpha_{\text{peak}} = \frac{3.0 \times 10^{-19} \times 1.7 \times 10^{14} \text{ cm}^{-1}}{0.046 \text{ cm}^{-1}} = 1.1 \times 10^{-3}, \quad (2)$$

and the fractional transmission against a bright continuum background source is then $\tau_{\text{peak}} = e^{-\alpha_{\text{peak}}} = 0.999$. Therefore, a detection at the 3σ level requires a signal-to-noise ratio in the continuum of $\sim$2700. Although the high-resolution spectrograph CRIRES at the VLT could obtain spectra with signal-to-noise ratios of a few hundreds routinely, and values in excess of 5000 have been reported (Smoker 2017), it is clear that a potential detection of this line in the IR from the ground will be quite challenging. Also, instruments like ISHELL at Maunakea or the upcoming CRIRES+ at the VLT (also METIS at the Extremely Large Telescope and GMTNIRS at the Giant Magellan Telescope in the not so distant future) could provide the necessary sensitivity to detect these lines. The lines of sight would be those of diffuse clouds in front of bright IR sources, like the dust envelopes around massive star formation regions. Other possible environments like dense PDRs can have CH^+ column densities that are $\sim$100 times higher, although the higher excitation temperatures would decrease the intensity of individual lines because of increased partitioning of the population. At an excitation temperature of 500 K, the strongest absorption would be that of the $R(3)$ line, with about one-tenth of the total intensity. Depending on the velocity structure and spread of the cloud, a detectable absorption could also be feasible. Given the low vibrational transition dipole moment, millimeter-wave and vis-UV observations provide much better sensitivity for the study of this molecule in space. Notwithstanding the difficulties, IR observations will always be complementary, since they can target different sources, and with higher spatial resolution than millimeter-wave ones. Moreover, millimeter-wave observations from the ground are quite difficult for the $J = 1-0$ line of $^{13}CH^+$ and impossible for $^{12}CH^+$, making IR observations a potential future tool to contribute to the understanding of the processes at work in the regions where this ion is formed.

This work (including the research visit of J.L.D. to Köln) has been supported by the Deutsche Forschungsgemeinschaft (DFG) via SFB 956 project B2 and the Gerätezentrum "Cologne Center for Terahertz Spectroscopy." J.L.D. acknowledges partial support from the Spanish MINECO through grant FIS2016-77726-C3-1-P and from the European Research Council through grant agreement ERC-2013-SyG-610256 NANOCOSMOS. The authors thank Sandra Brünken for discussions and Holger Müller and Volker Ossenkopf-Okada for reading the manuscript before publication.

Noted Added in Proof. A work describing a Dunham fit of the available frequencies of all CH^+ isotopologues has recently been submitted by Yu et al. (2018).

ORCID iDs

José L. Doménech https://orcid.org/0000-0001-8629-2566
Stephan Schlemmer https://orcid.org/0000-0002-1421-7281
Oskar Asvany https://orcid.org/0000-0003-2995-0803

References

Agúndez, M., Goicoechea, J. R., Cernicharo, J., Faure, A., & Roueff, E. 2010, ApJ, 713, 662
Amano, T. 2010a, ApJL, 716, L1
Amano, T. 2010b, JChPh, 133, 244305
Asvany, O., Bielau, F., Moratschke, D., Krause, J., & Schlemmer, S. 2010, RScI, 81, 076102
Asvany, O., Brünken, S., Kluge, L., & Schlemmer, S. 2014, ApPhB, 114, 203
Asvany, O., Krieg, J., & Schlemmer, S. 2012, RScI, 83, 093110
Bembenek, Z. 1997a, JMoSp, 181, 136
Bembenek, Z. 1997b, JMoSp, 182, 439
Bembenek, Z., Cisak, H., & Kepa, R. 1987, JPhB, 20, 6197
Brünken, S., Kluge, L., Stoffels, A., Asvany, O., & Schlemmer, S. 2014, ApJL, 783, L4
Brünken, S., Kluge, L., Stoffels, A., Pérez-Ríos, J., & Schlemmer, S. 2017, JMoSp, 332, 67
Carrington, A., & Ramsay, D. 1982, PhyS, 25, 272
Cernicharo, J., Liu, X.-W., González-Alfonso, E., et al. 1997, ApJL, 483, L65
Cheng, M., Brown, J., Rosmus, P., et al. 2007, PhRvA, 75, 012502
Cho, Y.-S., & Le Roy, R. J. 2016, JChPh, 144, 024311
Cueto, M., Cernicharo, J., Barlow, M. J., et al. 2014, ApJL, 783, L5
Dalgarno, A. 1976, in Atomic Processes and Applications, ed. P. G. Burke (Amsterdam: North-Holland), 109
Doménech, J. L., Drouin, B. J., Cernicharo, J., Herrero, V. J., & Tanarro, I. 2016, ApJL, 833, L32
Doménech, J. L., Schlemmer, S., & Asvany, O. 2017, ApJ, 849, 60
Douglas, A. E., & Herzberg, G. 1941, ApJ, 94, 381
Dunham, T. 1937, PASP, 49, 26
Endres, C. P., Schlemmer, S., Schilke, P., Stutzki, J., & Müller, H. S. P. 2016, JMoSp, 327, 95
Falgarone, E., Ossenkopf, V., Gerin, M., et al. 2010, A&A, 518, L118
Falgarone, E., Phillips, T. G., & Pearson, J. C. 2005, ApJL, 634, L149
Falgarone, E., Zwaan, M., Godard, B., et al. 2017, Natur, 548, 430
Flower, D. R., & Pineau des Forets, G. 1998, MNRAS, 297, 1182
Follmeg, B., Rosmus, P., & Werner, H.-J. 1987, CPL, 136, 562

Godard, B., Falgarone, E., Gerin, M., et al. 2012, A&A, 540, A87
Godard, B., Falgarone, E., & Pineau des Forêts, G. 2014, A&A, 570, A27
Hakalla, R., Kępa, R., Szajna, W., & Zachwieja, M. 2006, EPJD, 38, 481
Hierl, P. M., Morris, R. A., & Viggiano, A. A. 1997, JChPh, 106, 10145
Hobbs, L. M., Thorburn, J. A., Oka, T., et al. 2004, ApJ, 615, 947
Jusko, P., Konietzko, C., Schlemmer, S., & Asvany, O. 2016, JMoSp, 319, 55
Jusko, P., Stoffels, A., Thorwirth, S., et al. 2017, JMoSp, 332, 59
Lesaffre, P., Pineau des Forêts, G., Godard, B., et al. 2013, A&A, 550, A106
Menten, K. M., Wyrowski, F., Belloche, A., et al. 2011, A&A, 525, A77
Müller, H. S. P. 2010, A&A, 514, L6
Muller, S., Müller, H. S. P., Black, J. H., et al. 2017, A&A, 606, A109
Nagy, Z., Van der Tak, F. F. S., Ossenkopf, V., et al. 2013, A&A, 550, A96
Parikka, A., Habart, E., Bernard-Salas, J., et al. 2017, A&A, 599, A20
Pearson, J. C., & Drouin, B. J. 2006, ApJL, 647, L83
Rehfuss, B. D., Jagod, M.-F., Xu, L.-W., & Oka, T. 1992, JMoSp, 151, 59
Sauer, S. P. A., & Paidarová, I. 1995, CP, 201, 405
Sauer, S. P. A., & Špirko, V. 2013, JChPh, 138, 024315
Savić, I., Gerlich, D., Asvany, O., Jusko, P., & Schlemmer, S. 2015, MolPh, 113, 2320
Smoker, J. 2017, in 2017 ESO Calibration Workshop: The Second Generation VLT Instruments and Friends (ESOCal2017) (Santiago: ESO), https://doi.org/10.5281/zenodo.887307
Stoffels, A., Kluge, L., Schlemmer, S., & Brünken, S. 2016, A&A, 593, A56
Töpfer, M., Jusko, P., Schlemmer, S., & Asvany, O. 2016, A&A, 593, L11
Valdivia, V., Godard, B., Hennebelle, P., et al. 2017, A&A, 600, A114
Welty, D. E., Federman, S. R., Gredel, R., Thorburn, J. A., & Lambert, D. L. 2006, ApJS, 165, 138
Weselak, T., Galazutdinov, G., Musaev, F., & Krełowski, J. 2008, A&A, 479, 149
Western, C. M. 2017, JQSRT, 186, 221
Yu, S., Drouin, B. J., Pearson, J. C., & Amano, T. 2015, in 70th International Symposium on Molecular Spectroscopy (Urbana, IL: ISMS), https://dx.doi.org/10.15278/isms.2015.RD06
Yu, S., Drouin, B. J., Pearson, J. C., & Amano, T. 2016, in 71st International Symposium on Molecular Spectroscopy (Urbana, IL: ISMS), https://dx.doi.org/10.15278/isms.2016.MH01
Yu, S., Drouin, B. J., Pearson, J. C., & Amano, T. 2018, JMoSp, submitted
Zanchet, A., Godard, B., Bulut, N., et al. 2013, ApJ, 766, 80